

# GRAVLITE II: Non-parametric modelling of dwarf spheroidals

P. Steger<sup>1\*</sup>, J. I. Read<sup>1,2</sup>

<sup>1</sup>*Institute for Astronomy, Department of Physics, ETH Zürich, Wolfgang-Pauli-Strasse 27, CH-8093 Zürich, Switzerland*

<sup>2</sup>*Department of Physics, University of Surrey, Guildford, GU2 7XH, UK*

27 October 2014

## ABSTRACT

We show applications of the new mass modelling tool Gravlite to observed dwarf galaxies, Fornax, Sculptor, Sextans, Carina, and Draco.

**Key words:** galaxies: dwarf – galaxies: fundamental parameters – galaxies: kinematics and dynamics – cosmology: dark matter

## 1 INTRODUCTION

## 2 METHOD

We employ the non-parametric mass modelling described in (?):

The total mass density is given in bins by

$$\rho_{\text{tot}} = \text{TODO} \quad (1)$$

### 2.1 Splitting Populations

Observations of the abundances of metals and chemical species in the stellar atmospheres show that the ensemble of stars in a dwarf galaxy or globular cluster can be split into populations.

The first approach by Walker & Peñarrubia (2011) showed that if the population of e.g. Fornax is split into two populations, and each of their half-light radius and mass are determined, restrictions on the overall potential can be drawn. Using this approach, they prefer a cored DM profile for Fornax.

For real data, we will use a splitting based on metallicity. This is achieved by using a separate Markov Chain Monte Carlo method. The overall metallicity distribution is represented by a sum of two Gaussians with means  $\mu_{1,2}$  and widths  $\sigma_{1,2}$ , and each stellar tracer with metallicity  $M$  is assigned a population based on the likelihood of its metallicity belonging to said population. The process is repeated to marginalize over the means and widths of the metallicity distributions. A sample splitting result is shown in fig. 1.

In our test suite there are dwarf galaxies with different scale radii and small differences in the mean of the metallicity for the two populations of stars. In order to reproduce

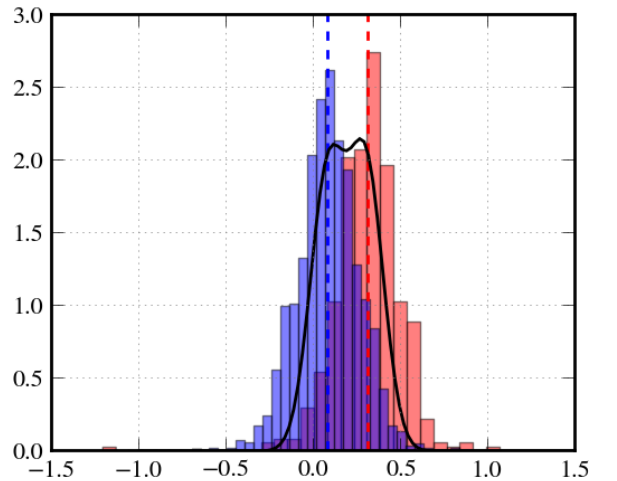


**Figure 1.** Reconstruction of two populations from mock data. The underlying metallicity distributions are shown as red and blue histograms. The retrieved centers of the Gaussians are shown as vertical lines, and the reconstructed metallicity distribution is depicted as black line.

the underlying populations we use an inset MCMC with assumptions that

- (i) Foreground stars are younger than most of the dSph member stars. Therefore, they show a high metallicity and can be removed from the dataset with a single cut in metallicity;
- (ii) the remaining stellar components are divided into two populations;
- (iii) the fraction of stars in population 1 is sampled in a uniform way in the range  $[0.2, 0.8]$ ;

\* E-mail: psteger@phys.ethz.ch

(iv) both populations show a normal distribution in metallicity with the same width;

(v) the initial values of the means are set to half and twice the mean metallicity, to allow for a reasonable difference between the means. This difference is then subsequently sampled assuming a normal distribution;

(vi) 40000 iterations for burn-in and 10000 iterations for subsequent parameter estimates are used, with a thinning by factor 10 to reduce correlations between subsequent models. This procedure converges in all tested cases.

To test whether the assignment into populations is a valid one, we want to check whether the population is in equilibrium with the overall potential.

The routine then assigns each particle to one of the two populations, based on its Mg metallicity.  $75 \pm 4\%$  of all stars are assigned to the correct underlying distribution. This in turn changes the half-light radius by 110pc and  $-62$ pc for initial 390 pc, 730 pc half light radii. These changes are rather high, but the two populations still show distinct half-light radii.

We explicitly assume two populations of stellar tracers in dwarf galaxies, each with Gaussian distributions in metallicity with means  $\mu_1, \mu_2$ . Without requiring a minimum distance  $\delta\mu = \mu_2 - \mu_1$  between them, a representation with  $\mu_1 \approx \mu_2$  can be found. This model shows a higher  $\chi^2$  than other models and is thus disfavoured, but cannot be rejected from a Kolmogorov-Smirnov test on a  $p < 0.05$  basis.

Here we show the influence of setting a prior minimal  $\delta\mu_{\min}$  on the goodness of fit, and the allowed range of  $\delta\mu$ . We work on the metallicity distribution of one of the mock dwarfs with cusped density profiles described earlier on, setting

$$\mu_1 \in [-1.0, 2.0]; \quad \delta\mu \in [\delta\mu_{\min}, 5.0]; \quad (2)$$

with  $\delta\mu_{\min}$  varying from 0.0 to 0.4. We let the MCMC run for a) 10k iterations with 8k burn-in/discarded models; b) 50k iterations with 40k burn-in. From the accepted models, we compute the mean Gaussian distributions and compare the corresponding overall bimodal distribution to the actual metallicity distribution from the data with a 2 component Kolmogorov-Smirnov test, and take the two-tailed statistics  $p_{KS}$  from 30 drawings. If  $p_{KS} > 0.05$ , then we cannot reject the hypothesis that the distributions of the two samples are the same.

Results for varying the minimal distance between the two Gaussians between 0.0 and 0.4 are shown in fig. 3.

All models with  $p > 0.05$  give a reasonable fit, with a maximum for 10k iterations at around  $\delta\mu = 0.1$ . Models with  $\delta\mu > 0.2$  give no good fit anymore after 10k iterations.

The goodness of fit is enhanced if we take more iterations, so in the plot for 50k iterations, there is a maximum  $p = 0.79$  compared to  $p = 0.4$  from 10k iterations only. The whole curve is shifted to higher  $\delta\mu$  values. The models with  $\delta\mu > 0.3$  are rejected. The restriction of  $\delta\mu > 0.4$  (last point to the right) is well-fitting again, but this is due to the fact that the fraction of particles for population 2 was found to be smaller than 10 percent, thus mainly fitting the metallicity distribution with one Gaussian only, plus some skewing from an almost negligible stellar component. Although this model cannot be rejected, it lies above the rejected models

at  $\delta\mu_{\min} = 0.4$ . Furthermore, it does not yield a second component with a scale length distinctly different from the main component, rendering the additional gain from two components obsolete. Thus, we will restrict the MCMC search of the population fraction to the range  $f \in [0.3, 0.7]$ .

### 3 DATA

#### 3.1 Fornax

(TODO: ref) find evidence for three populations.

#### 3.2 Sculptor

#### 3.3 Carina

#### 3.4 Sextans

#### 3.5 Draco

#### 3.6 Photometric Tracer Densities

selection function as function of smoothing scale as given in Walker 2009

$$\text{photometric data} = 1/w * \text{kinematic sample}$$

### 4 RESULTS

TODO:  $\chi^2$  distribution, Sigma, sigma

TODO: Sextans

### 5 CONCLUSIONS

The new non-parametric method samples the profiles of the overall density bin-wise, and was shown to reconstruct the density of diverse mock data.

### 6 ACKNOWLEDGEMENTS

JIR would like to acknowledge support from SNF grant PP00P2\_128540/1.

### REFERENCES

Walker M. G., Peñarrubia J., 2011, ApJ, 742, 20

### 7 APPENDIX

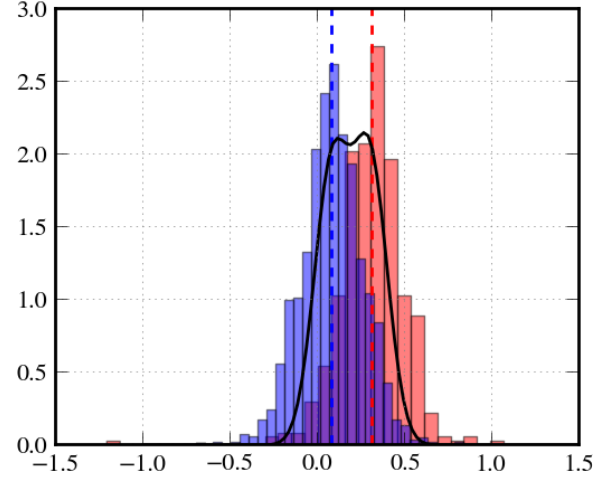


**Figure 2.** Distribution function of two populations (filled histograms) and the reproduced overall distribution.

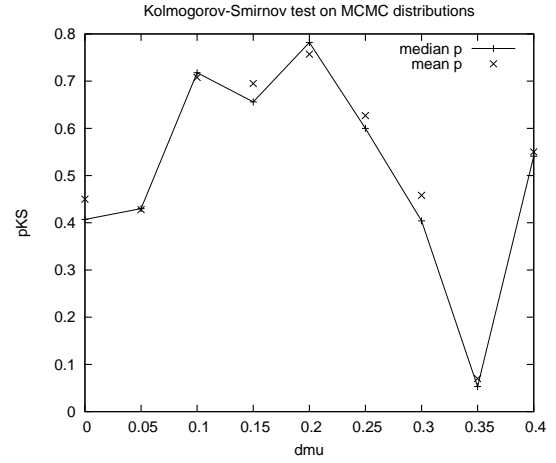
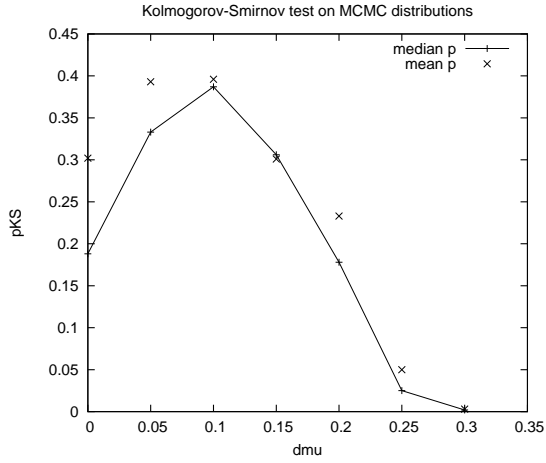


**Figure 3.** Kolmogorov-Smirnov test statistic  $p_{KS}$  for correspondence between models with  $\delta\mu > \delta\mu_{\min}$  as described in the text.

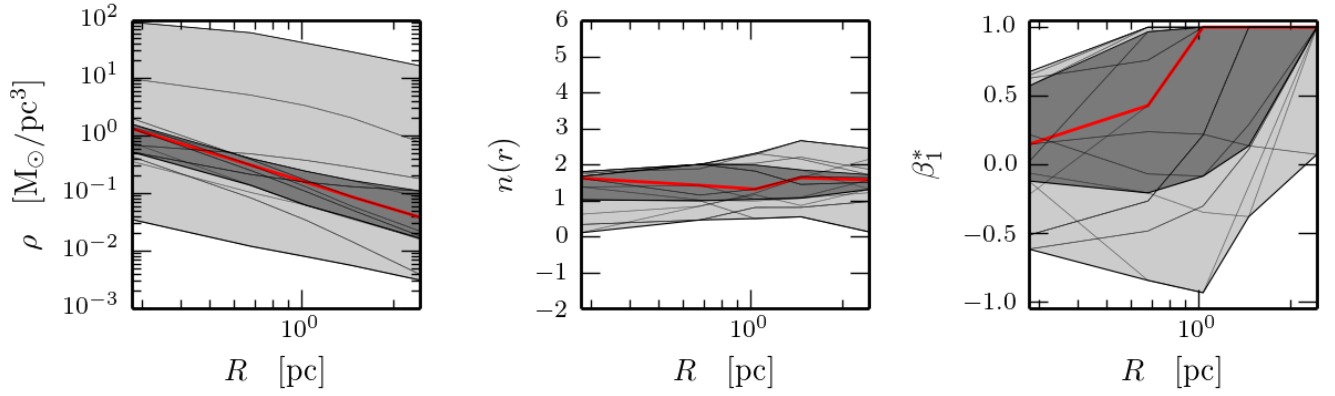


**Figure 4.** Reconstructed density, density slope, and velocity anisotropy of Fornax (red shows median, shaded areas show the 68 and 95 percentiles) for TODO tracer particles, after TODO iterations. The vertical lines give the projected half-light radius (for 2D quantities), and the half-light radius for the median model for 3D quantities.

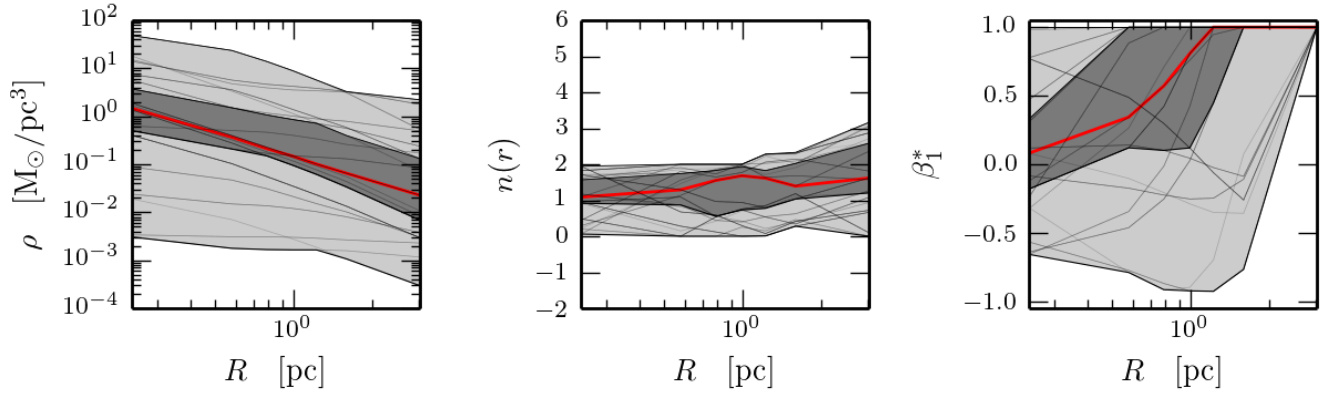


**Figure 5.** Reconstructed density, density slope, and velocity anisotropy of Carina (red shows median, shaded areas show the 68 and 95 percentiles) for TODO tracer particles, after TODO iterations. The vertical lines give the projected half-light radius (for 2D quantities), and the half-light radius for the median model for 3D quantities.

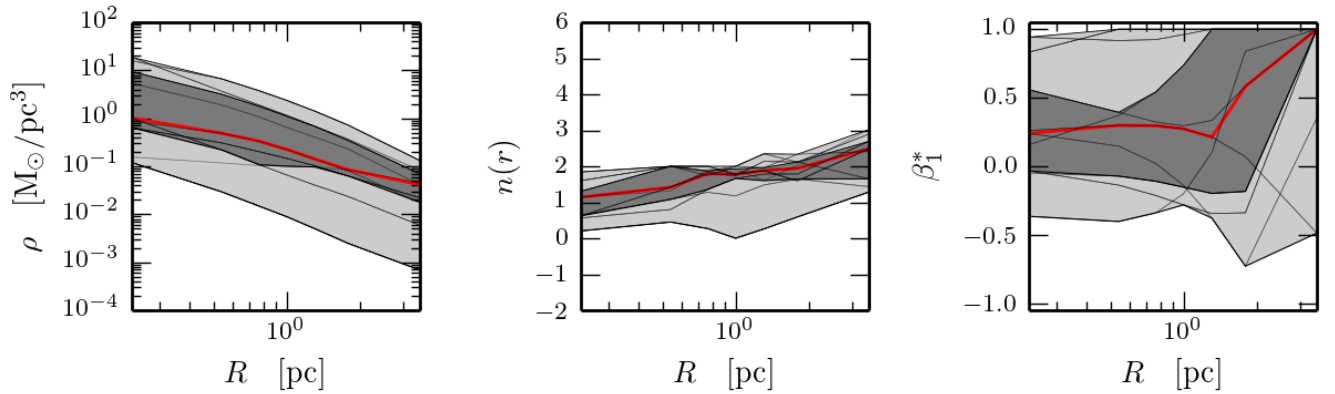


**Figure 6.** Reconstructed density, density slope, and velocity anisotropy of Sculptor (red shows median, shaded areas show the 68 and 95 percentiles) for TODO tracer particles, after TODO iterations. The vertical lines give the projected half-light radius (for 2D quantities), and the half-light radius for the median model for 3D quantities.